Vol 18 No 5, May 2009
1674-1056/2009/18(05)/1898-08

Chinese Physics B

© 2009 Chin. Phys. Soc.
and IOP Publishing Ltd

Concrete damage diagnosed using the non-classical nonlinear acoustic method*

Zhou Dao(周 到)[a], Liu Xiao-Zhou(刘晓宙)[a]†, Gong Xiu-Fen(龚秀芬)[a], Nazarov V E[b], and Ma Li(马 力)[c]

[a] *Key Laboratory of Modern Acoustics, Ministry of Education, Institute of Acoustics, Nanjing University, Nanjing* 210093, *China*
[b] *Institute of Applied Physics, Russian Academy of Science, Russian Federation*
[c] *Institute of Acoustics, Chinese Academy of Sciences, Beijing* 100190, *China*

(Received 6 May 2008; revised manuscript received 4 August 2008)

It is known that the strength of concrete is seriously affected by damage and cracking. In this paper, six concrete samples under different damage levels are studied. The experimental results show a linear dependence of the resonance frequency shift on strain amplitude at the fundamental frequency, and approximate quadratic dependence of the amplitudes of the second and third harmonics on strain amplitude at the fundamental frequency as well. In addition, the amplitude of the third harmonics is shown to increase with the increase of damage level, which is even higher than that of the second harmonics in samples with higher damage levels. These are three properties of non-classical nonlinear acoustics. The nonlinear parameters increase from 10^6 to 10^8 with damage level, and are more sensitive to the damage level of the concrete than the linear parameters obtained by using traditional acoustics methods. So, this method based on non-classical nonlinear acoustics may provide a better means of non-destructive testing (NDT) of concrete and other porous materials.

Keywords: concrete, non-classical nonlinear acoustics, non-destructive testing (NDT), crack
PACC: 4325

1. Introduction

Concrete, especially ultra-high performance concrete (UHPC), is well known as a complex multi-scale material.[1] The non-destructive testing (NDT) of concrete has attracted more attention because of its wide application. As a matter of fact, the NDT of concrete has many methods, such as the ultrasonic pulse method, the bounce elasticity method, the vibration method and the acoustical emission method. As is well known, the ultrasonic technique is an important means of NDT of concrete. However, so far, it is still based on linear parameters, such as sound speed and attenuation. In 1994, Popovics and Rose summarized the ultrasonic NDT of concrete.[2] Schubert and Marklein carried out a numerical simulation of ultrasonic wave propagation in concrete.[3] Ohdaira and Masuzawa researched the influence of water content on sound speed.[4] The strength of concrete, which is related to cracks, is a crucial index to evaluate concrete performance,[5,6] and it is also commonly considered to be the most important property of concrete. In some cases, conventional methods fail to provide a reliable means of the NDT of concrete. So, an improved method that can be used to more accurately estimate the strength of concrete is strongly desired.

Great interest has been aroused in nonlinear phenomena of solids due to their acoustic nonlinear characteristics. The feasibility of these methods is based on the known fact that acoustic properties are greatly dependent on structural defects, such as cracks, grains, dislocations, etc. Recent studies indicate that porous materials, such as rock and concrete, show strong acoustic nonlinearity.[7] Lacouture *et al*[8] studied the behaviour of concrete by using linear and nonlinear methods separately. The physical properties of concrete evolve significantly from the liquid state to the solid state. The results indicated that concrete was a kind of non-classical hysteretic elastic material the same as rock. Bentahar *et al*[9] studied the fast and slow dynamics in concrete. The hardening of concrete, caused by the reaction of hydration of the cement, is a well-studied process.[10] Furthermore, it is known that the nonlinear properties of hardened

*Project supported by the National Natural Science Foundation of China (Grant No 10674066) and the Open Project in State Key Laboratory of Acoustics (Grant No 200802).
†Corresponding author. E-mail: xzliu@nju.edu.cn

concrete are closely related to the presence of microcracking in some manners.[11]

In the present paper, six pieces of concrete samples made from the same materials, i.e. they are identical in composition and content proportion, are damaged under different pressures. Sound speed, first resonance frequency and resonance frequency shift of the six samples are measured. Based on these results, an ultrasonic nonlinear method to estimate the concrete damage level by using non-classical nonlinear parameters is investigated. In addition, the possibility of its application to the NDT of structural imperfections and porous materials is also discussed.

2. General equation and solution

The Poisson's ratio of concrete is in a range about from 0.14 to 0.17,[12−14] which is smaller than that of ordinary metals. Thus, transverse expansion in the concrete sample is very weak. Longitudinal sound propagation along the x direction in the sample can be described approximately as follows:

$$\rho U_{tt} = \sigma_x(\varepsilon), \tag{1}$$

where U is the particle displacement in the sample, ρ is the material density of the sample, σ is the stress, ε is the strain and t is the time. The boundary conditions for acoustically rigid samples and one free boundary are expressed in the following form:

$$\begin{aligned} &U(0,t) = A_0\cos(\omega t),\\ &U_x(L,t) = 0, \end{aligned} \tag{2}$$

where A_0 is the amplitude of the wave produced by the source, L is the length of the sample and ω is the angular frequency.

The natural resonance frequencies of the sample can be determined from the above boundary conditions as[15,16]

$$F_n = F_1(2n-1), \quad F_1 = c/4L, \quad n = 1,2,\ldots, \tag{3}$$

where c is the longitudinal wave speed in the sample, and the positive integer n refers to the longitudinal mode number of the sample.

When $\sigma(\varepsilon) = E\varepsilon$ and $\varepsilon = \dfrac{\partial U}{\partial x}$, Eq.(1) is replaced by the following form:

$$U_{tt}{=}c^2U_{xx}, \tag{4}$$

where $c = \sqrt{E/\rho}$, with E being the Young's modulus of the sample.

In order to describe hysteresis and non-classical nonlinearity in the concrete sample, we assume the equation for describing the relationship between stress and strain in the sample to have the following form:[15]

$$\sigma(\varepsilon) = \begin{cases} E\left(\varepsilon - \dfrac{\gamma_1}{2}\varepsilon^2\right); & \varepsilon > 0, \quad \varepsilon_t > 0,\\ E\left(1 - \dfrac{\gamma_1}{2}\varepsilon_0\right)\varepsilon; & \varepsilon > 0, \quad \varepsilon_t < 0,\\ E\left(\varepsilon + \dfrac{\gamma_2}{2}\varepsilon^2\right); & \varepsilon < 0, \quad \varepsilon_t < 0,\\ E\left(1 - \dfrac{\gamma_2}{2}\varepsilon_0\right)\varepsilon; & \varepsilon < 0, \quad \varepsilon_t > 0, \end{cases} \tag{5}$$

where ε_0 is the strain amplitude, and the nonlinear parameters γ_1 and γ_2 describe the small deviation from Hook's law. Here, $\gamma_1 \neq \gamma_2$, which reflects the asymmetry of the compression and expansion processes.

Substituting expression (5) into Eq.(1), the following equation can be obtained:

$$U_{tt} - c^2U_{xx} = c^2F(U), \tag{6}$$

where $F(U)$ can be determined by the following expression:

$$F(U) = \begin{cases} -\gamma_1U_xU_{xx}; & U_x > 0, \quad U_{xt} > 0,\\ -\dfrac{\gamma_1}{2}(\varepsilon_0U_{xx} + \varepsilon_{0x}U_x); & U_x > 0, \quad U_{xt} < 0,\\ \gamma_2U_xU_{xx}; & U_x < 0, \quad U_{xt} < 0,\\ -\dfrac{\gamma_2}{2}(\varepsilon_0U_{xx} + \varepsilon_{0x}U_x); & U_x < 0, \quad U_{xt} > 0, \end{cases} \tag{7}$$

where $\varepsilon_{0x} = \dfrac{\partial\varepsilon_0}{\partial x}$.

To take nonlinear viscous loss into consideration, the term μU_{ttt} should be introduced, where μ is the viscous coefficient. Equation (6) can be substituted by the following expression:

$$U_{xx} - c^2U_{xx} + \mu U_{ttt} = c^2F(U). \tag{8}$$

To facilitate the analysis, we invoke the substitution

$$V(x,t) = U(x,t) - A_0\cos(\omega t)(1 + \sin(k_nx)), \tag{9}$$

where $k_n = 2\pi f_n/c$ is the natural wave number of the resonator in the linear approximation. Now, the boundary conditions have the form

$$V(0,t) = V_x(L,t) = 0. \tag{10}$$

Considering the vibration of the sample near the resonance of the n-th mode and the boundary conditions, while the excitation amplitude is as small as $A_0 \ll U_0$, where U_0 is the amplitude of displacement

at the resonance frequency in the sample, the following equation can be obtained:[15]

$$\begin{aligned} & V_{tt} - c^2 V_{xx} \\ = \; & c^2 F(V) - \mu V_{tt} \\ & + A_0\{\omega^2 + (\omega^2 - \omega_n^2)\sin(k_n x)\}\cos(\omega t). \end{aligned} \quad (11)$$

The right-hand side of the above equation contains terms describing the nonlinearity, dissipation, and the external force. Assuming that these terms are small compared with the amplitude of the resonator, we seek a solution having the form of the homogeneous equation:

$$V^{(1)} = V_0 \cos[(\omega_n + \delta)t + \psi]\sin(k_n x) + W(x,t), \quad (12)$$

where V_0 and ψ are the displacement amplitude and the phase for the sample at the frequency of the external force, ω, respectively, W is a small increment, and $\delta = \omega - \omega_n$, which means that the resonance frequency shift is much smaller than ω_n. The sample strain amplitude is determined by the expression[15]

$$V_0 = \frac{A_0(c/L)}{[(\delta - \delta_n)^2 + (\mu_1 + \mu_n)^2\omega_n^2/4]^{1/2}}, \quad (13)$$

$$\begin{aligned} & \delta_n = -2(n - 1/2)a_1 V_0 \omega_n / 3L, \\ & \mu_n = 4(n - 1/2)b_1 V_0 / 3L\omega_n, \\ & a_1 = \frac{(8 + 3\pi)(\gamma_1 + \gamma_2)}{12\pi}, b_1 = \frac{\gamma_1 + \gamma_2}{6\pi}, \end{aligned} \quad (14)$$

where δ_n and μ_n are the resonance frequency shift and the nonlinear loss factor, respectively. $\mu_1 = (\omega_1 Q_1)^{-1}$ with Q_1 being the quality factor of the first mode.

The components at the second and third harmonic frequencies can be separated out by using the perturbation method. The second harmonics is not resonant for the given resonator when the sample is resonant. It is well known that losses can be neglected in the exciting of a resonator far from resonance, and so we can set $\mu_2 = 0$. The third harmonics is resonant because of the odd resonant frequencies of the sample. The μ_3 must be introduced in the calculation. The displacement amplitude at the second and third harmonic frequencies for resonant excitation at the fundamental frequency can be written as follows:[15]

$$\begin{aligned} & V_2(x) \\ = \; & \frac{V_0^2 k_n \sqrt{a_2^2 + b_2^2}}{32}(\sin(2k_n x) - 2k_n x\cos(2k_n x)), \end{aligned} \quad (15)$$

where $a_2 = \dfrac{(8 + 3\pi)(\gamma_1 - \gamma_2)}{24\pi}$, and $b_2 = \dfrac{\gamma_1 - \gamma_2}{6\pi}$.

The amplitude of V_2 at the free end ($x = L$) can be expressed as

$$V_2(x = L) = \frac{V_0^2 k_n^2 L}{16}\sqrt{a_2^2 + b_2^2}, \quad (16)$$

and

$$\begin{aligned} & V_3(x = L) \\ = \; & \frac{2(n - 1/2)}{45L}\frac{V_0^2 \omega_n \sqrt{a_3^2 + b_3^2}}{[9\mu_3^2\omega_n^4 + 4(1 - 27a_0/35a_1)^2\delta_n^2]^{1/2}}, \end{aligned} \quad (17)$$

where $\mu_3 = (\omega_3 Q_3)^{-1}$, $a_0 = \dfrac{(\pi + 4)(\gamma_1 + \gamma_2)}{8\pi}$, $a_3 = \dfrac{2(\gamma_1 + \gamma_2)}{15\pi}$, and $b_3 = \dfrac{\gamma_1 + \gamma_2}{30\pi}$. V_2 and V_3 represent the displacements at the second and third harmonics, respectively.

From the resonance frequency shift and the amplitudes of the first three harmonics at the free end of the sample ($x = L$), the values of the parameters $|\gamma_1 - \gamma_2|$ and $\gamma_1 + \gamma_2$ at the first resonance mode can be worked out as follows:

$$|\gamma_1 - \gamma_2| = \frac{16^* V_2}{V_0^2 k_n^2 L\sqrt{\left(\dfrac{8 + 3\pi}{24\pi}\right)^2 + \left(\dfrac{1}{6\pi}\right)^2}}, \quad (18)$$

$$\gamma_1 + \gamma_2 = \frac{45LV_3\sqrt{9u_3^2\omega_n^4 + 4\left(1 + \dfrac{81(4 + \pi)}{70(8 + 3\pi)}\right)^2\delta_n^2}}{(2n - 1)\omega_n V_0^2\sqrt{\left(\dfrac{2}{15\pi}\right)^2 + \left(\dfrac{1}{30\pi}\right)^2}}. \quad (19)$$

3. Experimental technique

The experimental setup is schematically shown in Fig.1. The damaged sample was located above the transmitting transducer and Vaseline was chosen as a coupling medium in between. The transmitting transducer was cemented to a massive metallic loading mass. Moreover, the sample face, which contacted the emitter, was bound tightly to the experimental bracket. Therefore, the boundary condition at this end was considered to be close to that of an absolutely rigid sample, and the concrete sample was tightly fixed to the transmitting transducer. An accelerometer was set above another end of the sample, and oil was chosen as a couplant. A 0.09 kg cylindrical brass block was mounted above the accelerometer to make a good contact between the accelerometer and the sample. The total weight of the accelerometer and the brass block was so small that the corresponding sample boundary was considered to be acoustically soft. During the whole experiment, the relative positions between the transducer, the sample and the accelerometer were kept unchanged.

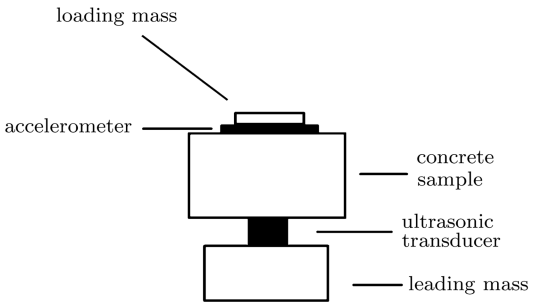


Fig.1. Experimental setup.

A tone-burst signal with a central frequency of 10.0 KHz, a burst of 50 cycles, and a pulse repetition frequency of 100 Hz, was produced from a waveform generator (Agilent 33250, Loveland, CO, USA), the exciting signal was fed into a power amplifier (ENI A150, Rochester, NY, USA). The output of the amplifier was applied to a transmitting transducer and the acoustic wave arriving at another end of the sample was detected by an accelerometer (PCB PIEZOTRONICS, ICP, USA). The transmitting transducer is lead zirconate titanate (PZT) with a diameter of 28 mm, made by Shantou Ultrasonic Co., Ltd., China. The receiving sensitivity of the accelerometer is 10 mV/g (1.02 mV/(m/s^2)) and its – 3 dB frequency range is from 5 Hz to 100 kHz. The received acceleration was recorded by a digital oscilloscope (Agilent 54810, Colorado Springs, CO, USA). The relationship between the measured acceleration (a) and the displacement amplitude of the sample (U_0) at the frequency of the external force, ω, is $U_0 = \frac{a}{\omega^2}$. In general, the resonance frequency for the acceleration of the sample is not equal to the resonance frequency for the displacement. The displacement resonance frequency of a sample is $f_r = f_0\sqrt{1-\frac{1}{2Q^2}}$, where f_0 is the natural frequency of the sample and Q is the quality factor. The acceleration resonance frequency of a sample is $f_s = Qf_0\sqrt{\frac{2}{2Q^2-1}}$. If the quality factor is large enough, f_r and f_s are nearly equal to f_0. From the following experimental results, the Q-factor of the concrete samples is large; therefore, the results of the resonance frequency measured by the accelerator can reflect the displacement resonance frequency of the samples.

The second harmonics of the transmitter was 35 dB lower than that of the first harmonics when the acoustic power was less than 1 W. The third harmonics was much lower. In fact, when the acoustic power was as low as 1 W, the nonlinear effect of the transmitter was so weak that it can be neglected.

Six concrete samples used in this paper were cubic shaped by $8 \times 6 \times 5\,\mathrm{cm}^3$. The weight ratio of cement to sand to carpolite was 1 : 2.46 : 4.19. 1.8 ton water was injected into one cubic meter of concrete. After the sample dried under the sun, the density of the concrete sample was 2400 kg/m^3 and the sound speed of the intact sample was 2900 m/s. Six samples were pressed under a 100 ton fatigue testing machine to make flaws. Since the maximal endurance pressure for this kind of concrete sample is 21 MPa, these six samples were pressed under 3.5, 7, 10.5, 14, 17.5, and 21 MPa, separately. Two pressed faces along the thickness direction were smoother than the other four faces, which were distorted a little; therefore the experiments in the present paper are performed in a longitudinal mode along the thickness direction.

Sound speeds for the six concrete samples were measured by the pulse transmission technique at the first natural resonance frequency of the sample, the frequency at which the receiving signal was biggest.

To measure the change of resonance frequency shift, the second and third harmonics dependences on the first harmonics, the emitting voltage applied to the transmitter was increased from 30 to 300 mV in steps of 30 mV. In order to compare the changes of the first three harmonics of the six concrete samples, a power spectrum was used to analyse the received signals. The value of the strain can be acquired directly from the acceleration.

4. Experimental results and discussion

The first sample under 3.5 MPa pressure suffered slight breakage and was almost intact. The second, third and fourth samples were more seriously damaged and the fifth and sixth samples, especially the latter one pressed under 21 MPa pressure, were the most damaged.

Table 1 gives the linear parameters of the six samples, including sound speed, the first resonance frequency (F_1). As shown in Table 1, the longitudinal wave speed is smaller and sound speed becomes higher for the more seriously damaged sample. The sound speed of the first sample is almost 50% higher than that of the sixth sample. On the other hand, the first resonance frequency also decreases from 13.5 (first sample) to 8.4 kHz (sixth sample). Because the

upper end of the sample has a loading mass, this end is approximately considered as a free end theoretically. Therefore, the experimental values of the first natural frequency are a little higher than theoretical ones.

The first and third harmonics are close to resonance, therefore the losses must be considered. However, μ_1 and μ_3 are very difficult to measure directly.

Table 1. Linear parameters for the six samples.

sample	pressure /MPa	length /m	time relay /μs	sound speed /(m/s)	F_1/kHz theoretical values	F_1/kHz experimental values
1	3.5	0.0550	19.0	2894	13.2	13.52
2	7.0	0.0545	20.0	2725	12.5	13.45
3	10.5	0.0540	21.5	2547	11.6	11.63
4	14.0	0.0535	24.0	2230	10.4	11.57
5	17.5	0.0610	28.0	2178	8.8	8.88
6	21.0	0.060	30.0	2033	8.3	8.39

According to the relationship between the nonlinear losses and the Q-factor discussed above, the Q-factor can reflect nonlinear losses indirectly. The Q-factor, whose values are different in different samples, also changes with the exciting force. As shown in Table 2, the values of the Q-factor at different strains are different for the sixth sample.

Table 2. Q-factor versus strain amplitude for the sixth sample.

strain amplitude	Q-Factor (–3 dB)
3.74×10^{-8}	66.7
7.64×10^{-8}	65.3
1.219×10^{-7}	63.1
1.58×10^{-7}	61.5
2.12×10^{-7}	59.9
2.58×10^{-7}	57.1
3.04×10^{-7}	55.1
3.50×10^{-7}	53.4
3.94×10^{-7}	51.1
4.37×10^{-7}	49.6

From the results in Table 3, we can find that the resonance frequency shift at a 300 mV inputting voltage increases from 18 to 603 Hz with the increase of damage level. The first sample, which is damaged under a pressure of 3.5 MPa, is almost intact and has few cracks in it. The resonance frequency shift and the nonlinear parameters γ_1 and γ_2 are the smallest (Table 3). But for the second, third and fourth samples, which are more seriously damaged, the non-classical nonlinear performances become more distinctive. In fact, the fifth and sixth samples are damaged most seriously, of which the non-classical nonlinear performances are most obvious. If we suppose that γ_1 is larger than γ_2, the values γ_1 and γ_2 can be easily calculated (Table 3), that is, with the increase of the damage level of the concrete, the nonlinear parameters $|\gamma_1 - \gamma_2|$ and $\gamma_1 + \gamma_2$ increase by more than one hundred times; the nonlinear parameters γ_1 and γ_2 increase to as high as 10^8 and the value of $|\gamma_1 - \gamma_2|$ gradually reaches the level of 10^7. We find that the nonlinear parameters in Table 3 are more sensitive to the damage level of the concrete than the linear parameters in Table 1. All the above means that the more damaged the sample is, the greater the non-classical nonlinear effect of the sample will be.

Table 3. Resonance frequency shift and nonlinear parameters for the six samples.

sample	resonance frequency shift/Hz	$\lvert\gamma_1 - \gamma_2\rvert$	$\gamma_1 + \gamma_2$	γ_1	γ_2
1	18	2.02×10^5	1.56×10^6	8.81×10^5	6.79×10^5
2	56	2.40×10^5	1.63×10^6	9.35×10^6	6.95×10^5
3	85	6.9×10^5	3.56×10^6	2.13×10^6	1.44×10^6
4	222	1.19×10^5	8.70×10^6	4.95×10^6	3.76×10^6
5	450	2.42×10^7	2.57×10^8	1.46×10^8	1.16×10^8
6	603	3.04×10^7	5.78×10^8	3.27×10^8	2.74×10^8

Figure 2 exhibits the power spectra for the six samples. From Fig.2(a), we find that the non-classical nonlinear effect is so weak that the amplitude of the third harmonics is still lower than that of the second harmonics for the first sample. With the increase of the damage level, the third harmonics increases, that is to say, the non-classical nonlinear effect becomes greater. The amplitude of the third harmonics is almost the same as that of the second harmonics for the second sample (Fig.2(b)). For a more damaged sample, the difference between the second harmonics and the third harmonics becomes larger and larger. As for the sixth sample (Fig.2(f)), the amplitude of the odd harmonics is higher than that of the even harmonics, which is a remarkable feature of the non-classical nonlinear phenomenon.

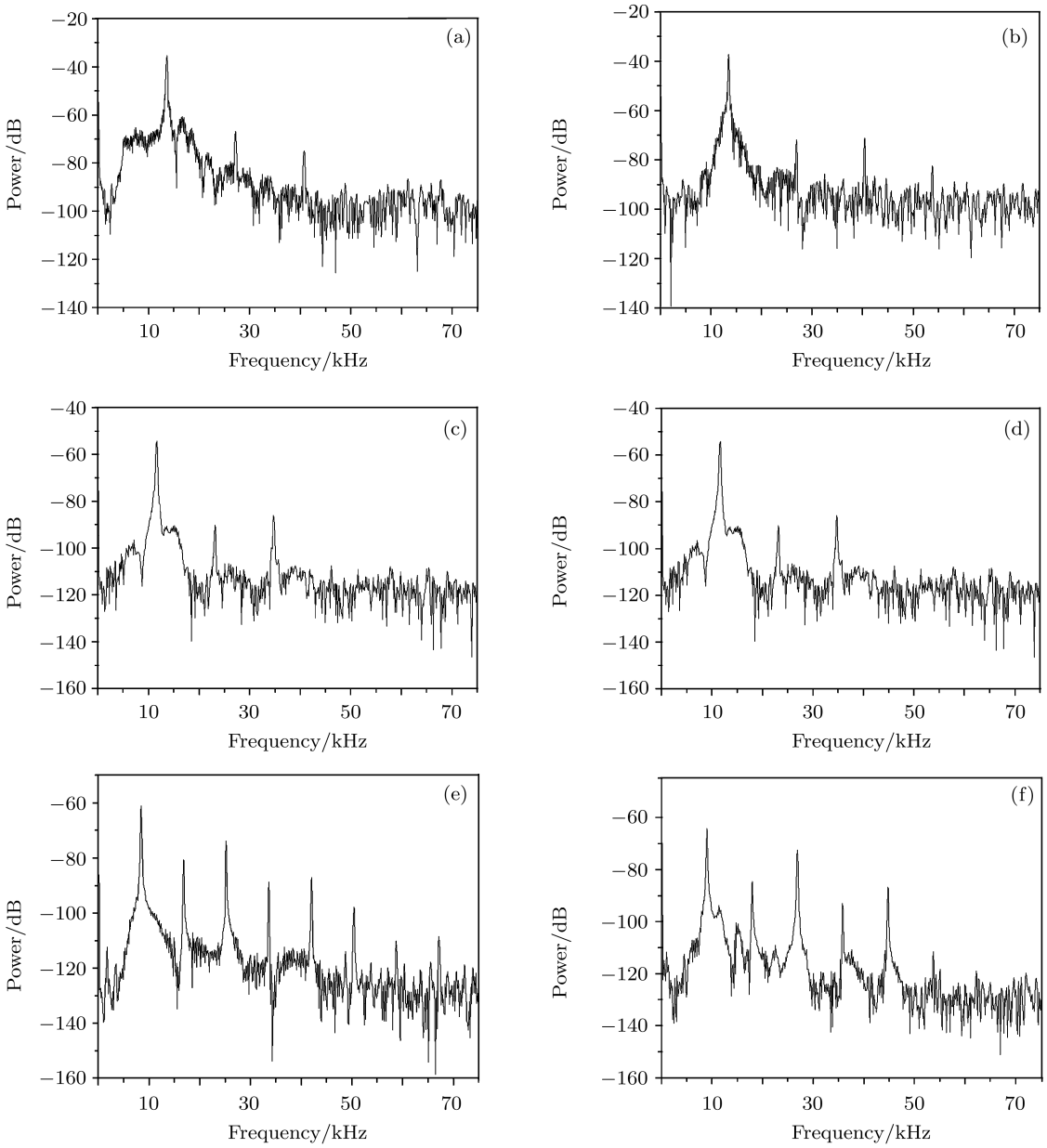


Fig.2. Power spectra of accelerations at free ends of the first (a), second (b), third (c), fourth (d), fifth (e) and sixth (f) samples.

From the comparison of change degree between the linear parameters (Table 1) and the nonlinear parameters (Table 3), we find that the resonance frequency shift and the nonlinear parameters change more distinctively in the damaged samples. In other words, the nonlinear parameters are more sensitive to the detecting of damage level of the concrete than the linear parameters.

Figure 3 shows the resonance frequency shifts as a linear function of the strain amplitude at the fundamental frequency for the first and sixth concrete samples. The resonance frequency of the sample decreases as strain increases. The resonance frequency shift ΔF describes the resonance frequency varying with the strain. Here $\Delta F = F - F_1$, with F and F_1 being resonance frequencies of the sample with and without strain, respectively. The experimental results also prove the linear relationship between the resonance frequency and the strain of the first harmonics as described in Eq.(14).

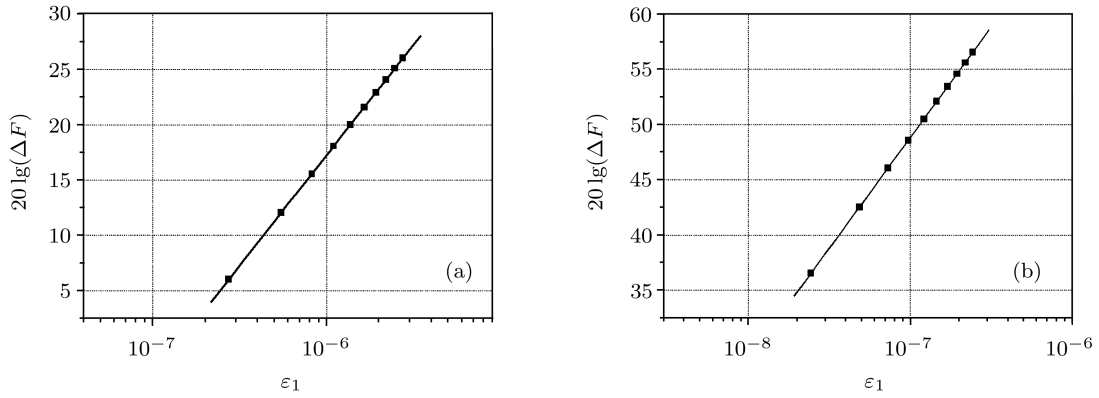


Fig.3. Resonance frequency shifts versus the first harmonic strain of the first (a) and sixth (b) concrete samples, where the solid lines represent first order fitting curves.

According to classical nonlinear theory, the amplitude of the third harmonics varies cubically with the first harmonics. On the other hand, in the non-classical nonlinear theory, the amplitude of the third harmonics is quadratically related to the amplitude of the first harmonics. Figure 4 describes that the second and third harmonics increase with the increase in strain amplitude at the fundamental frequency for the sixth sample. From the slopes of these two curves, we can obtain a quadratic relationship between the second and third harmonics and the first harmonics. Therefore, we can conclude that the concrete samples show the properties of non-classical nonlinear acoustics.

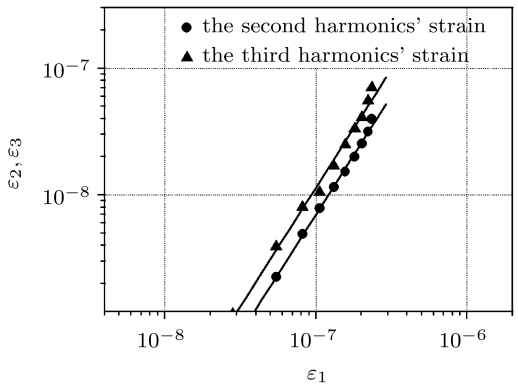


Fig.4. Variations of the second and third harmonic strains with the first harmonic strain for the sixth concrete sample, where the solid lines represent first order fitting curves.

5. Conclusions

In this paper, we have observed non-classical nonlinear phenomena in concrete samples. It is found that the nonlinear parameters are more sensitive to the damage level of concrete than the linear parameters. The amplitude levels of the third harmonics are approximately in proportion to the degree of damage. Therefore, the method based on non-classical nonlinear acoustics can provide an efficient way to assess concrete damage level. In addition, this may be extended to the NDT of other materials with strong non-classical nonlinear properties, such as porous materials.

References

[1] Vernet C, Lukasik J and Prat E in: Aitein P C and Delagrave Y (editors) 1998 *Proc. Int. Symb. on HPC and RPC* **3** 17

[2] Popovics J S and Rose J L 1994 *IEEE Trans. on Ultrasonics, Ferroelectrics, and Frequency Control* **41** 140

[3] Schubert F and Marklein R 2002 *IEEE Ultrasonics Sym-*

posium (Munich) 799
[4] Ohdaira E and Masuzawa N 2000 *Ultrasonics* **38** 546
[5] Terill J M 1986 *Mag. Concrete Res.* **38** 220
[6] Shilston C M 1961 *Soc. Nondestruct. Testing* **19** 39
[7] Abeele K V and Visscher J D 2000 *Cem. Concr. Res.* **30** 1453
[8] Lacouture J C, Johnson P A and Cohen-Tenoudji F 2003 *J. Acoust. Soc. Am.* **113** 1325
[9] Bentahar M, Aqra H E1, Guerjouma R E1, Griffa M and Scalerandi M 2006 *Phys. Rev.* B **73** 0141161
[10] Schutter G D and Taerwe L 1995 *Cem. Concr. Res.* **25** 593
[11] Johnson P A 1999 *Mater. World* **7** 544
[12] Wang Z F 2003 *Engineering Mechanics* (Beijing: Science Press) p397
[13] Wang C X and Liu N 1998 *Industrial Construction* **6** 28
[14] Wang Y F and Liang Y J 2004 *Journal of Northern Jiao-Tong University* **1** 28
[15] Nazarov V E, Ostrovsky L A, Soustova I A and Sutin A M 1998 *Sov. Phys. Acoust.* **34** 284
[16] Nazarov V E and Kolpakov A B 2000 *J. Acoust. Soc. Am.* **107** 1915